Journal of Engineering Sciences
Vol 10, Issue 9, Sept /2019
ISSN NO:0377-9254

EFFICIENT DESIGN AND IMPLEMENTATION OF A BIDIRECTIONAL DC/DC CONVERTER WITH DUAL-BATTERY ENERGY STORAGE FOR HYBRID ELECTRIC VEHICLE SYSTEM

[1]M.RAVI KUMAR, [2]D.RAMESH BABU
[1]M.Tech Student, [2]Assistant Professor
Department of EEE
KAKINADA INSTITUTE OF TECHNOLOGICAL SCIENCES (KITS), RAMACHANDRAPURAM.

Abstract : This study develops a newly designed, patented, bidirectional dc/dc converter (BDC) that interfaces a main energy storage (ES1), an auxiliary energy storage (ES2), and dc-bus of different voltage levels, for application in hybrid electric vehicle systems. The proposed converter can operate in a step-up mode (i.e., low-voltage dual-source-powering mode) and a step-down (i.e., high-voltage dc-link energy-regenerating mode), both with bidirectional power flow control. In addition, the model can independently control power flow between any two low-voltage sources (i.e., low-voltage dual-source buck/boost mode). Herein, the circuit configuration, operation, steady state analysis, and closed-loop control of the proposed BDC are discussed according to its three modes of power transfer. Moreover, the simulation and experimental results for a 1-kW prototype system are provided to validate the proposed converter.

Keywords: Hybrid electric vehicle (HEV), Permanent magnet synchronous motor (PMSM), propotional integral (PI) controller, battery.

---

1. INTRODUCTION

Global climate change and energy supply is declining have stimulated changes in vehicular technology. Advanced technologies are currently being researched for application in future vehicles. Among such applications, fuel-cell hybrid electric vehicles (FCV/HEV) are efficient and promising candidates. In the past, Ehsani et al. studied the vehicles' dynamics to look for an optimal torque-speed profile of the electric propulsion system [1]. Emadi et al. discussed the operating properties of the topologies for different vehicles including HEV, FCV, and more electric vehicles [2] . Emadi et al. also integrated power electronics intensive solutions in advanced vehicular power system to satisfy huge vehicular load [3]. Schaltz et al. sufficiently divide the load power among the fuel cell stack, the battery, and the ultra capacitors based on two proposed energy-management strategies [4]. Thounthong et al. studied the influence of fuel-cell (FC) performance and the advantages of hybridization for control strategies [5]. Chan et al. reviewed electric, hybrid, and fuel-cell vehicles and focused on architectures and modeling for energy management [6]. Khaligh and Li presented energy-storage topologies for HEVs and plug-in HEVs (PHEVs). They also discussed and compared battery, UC, and FC technologies. Furthermore, they also addressed various hybrid ESSs that integrate two or more storage devices [7]. Rajashekara reviewed the current status and the requirements of primary electric propulsion components-the battery, the electric motors, and the power electronics system [8]. Lai et al. implemented a bidirectional dc/dc converter topology with two-phase and interleaved characteristics. For EV and dc-microgrid systems, the converter has an improved voltage conversion ratio [9]. Furthermore, Lai also studied a bidirectional dc to dc converter (BDC) topology which has a high voltage conversion ratio for EV batteries connected to a dc-microgrid system [10]. In FCV systems, the main battery storage device is commonly used to start the FC and to supply power to the propulsion motor [2], [3]. The battery storage devices improve the inherently slow response time for the FC stack through supplying peak power during accelerating the vehicle [7]. Moreover, it contains a high power-density component such as super capacitors (SCs) eliminates peak power transients during accelerating and regenerative braking [11]. In general, SCs can store regenerative energy during deceleration and release it during acceleration, thereby supplying additional power. The high power density of SCs prolong the life span of both FC stack and battery storage devices and enhances the overall efficiency of FCV systems [2]–[8], [12].

A functional diagram for a typical (FCV/HEV) power system is illustrated in Fig. 1 [4, 13]. The low-voltage FC stack is used as the main power source, and SCs directly connected in parallel with FCs. The dc/dc power converter is used to convert the FC stack voltage into a sufficient dc-bus voltage in the driving inverter for supplying power to the propulsion motor. Furthermore, ES1 with rather higher voltage is used as the main battery storage device for supplying peak power, and ES2 with rather lower voltage

could be an auxiliary battery storage device to achieve the vehicle range extender concept [13]. The function of the bidirectional dc/dc converter (BDC) is to interface dual-battery energy storage with the dc-bus of the driving inverter.

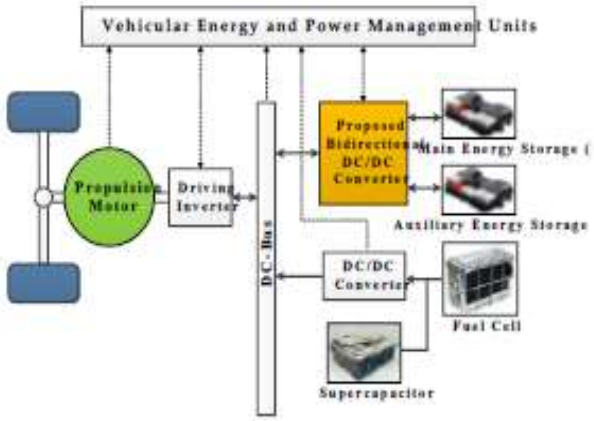

Fig. 1. Typical functional diagram for a FCV/HEV power system.

Generally, the FC stack and battery storage devices have different voltage levels. Several multiport BDCs have been developed to provide specific voltages for loads and control power flow between different sources, thus reducing overall cost, mass, and power consumption [14-27]. These BDCs can be categorized into isolated and nonisolated types.

In isolated converters, high-frequency power transformers are applied to enable galvanic isolation. A few isolated multiport BDC topologies have been investigated, such as the flyback, half- or full-bridge circuits, dual-active bridges, and resonant circuits [14-17, 20, 22, 24]. The literature suggests that nonisolated BDCs are more effective than typical isolated BDCs in EVs [18, 19, 21, 23, 25-27]. Liu *et al*. [18] derived nonisolated multi-input converter topologies by way of a combination of buck, boost, Ćuk, and Sepic. In [23], Wu *et al*. developed the three-port nonisolated multi-input-multi-output (MIMO) converter topologies for interfacing a renewable source, a storage battery, and a load simultaneously. The three double-input converters developed in [19] comprise a single-pole triple-throw switch and only one inductor. A modular nonisolated MIMO converter was presented in [26]. This converter is applied to hybridize clean energy sources of EVs and the basic boost circuit was modified and integrated. However, the voltage gain of the MIMO boost circuit is limited in practice, because of the losses associated with some components such as the main power switch, inductor, filter capacitor, and rectifier diode. To overcome this drawback, three-port power converter that has high-gain characteristic and contains FC, battery sources and stacked output for interfacing HEV, as well as a dc-microgrid was presented [27]. Although the multiport BDC discussed in [25] can interface more than two sources of power and operate at different voltage levels, itstill has limited static voltage gains, resulting in a narrow voltage range and a low voltage difference between the high-and low-side ports.

This study proposes a new BDC topology for FCV/HEV power systems that consists of an interleaved voltage-doubler structure [9, 28] and a synchronous buck-boost circuit. It features two main operating modes: a low-voltage dual-source-powering mode and a high-voltage dc-bus energy-regenerating mode. In addition, the proposed converter can independently control power flow between any two low-voltage sources when in the low-voltage dual-source buck/boost mode. A similar topology was introduced in [29] that only describes a brief concept. By contrast, this study presents a detailed analysis of the operation and closed-loop control of this new topology as well as simulation and experimental results for all its modes of operation. Moreover, this study expanded the topology presented in [29] because the proposed converter can operate over a wider range of voltage levels. The main characteristics of the proposed converter are summarized as follows: 1) interfaces more than two dc sources for different voltage levels, 2) controls power flow between the dc bus and the two low-voltage sources and also independently controls power flow between the two low-voltage sources, 3) enhances static voltage gain and thus reduces switch voltage stress, and 4) possesses a reasonable duty cycle and produces a wide voltage difference between its high- and low-side ports.

The remainder of this paper is structured as follows. The converter topology and operation principle are presented in Section II. The steady state characteristics of the converter, which are based on the operation principle, are analyzed in Section III, whereas Section IV presents the converter control scheme. A 1 kW converter prototype was constructed in this study to validate the proposed converter and demonstrate its merits. The corresponding simulated and experimental results are presented in Section V. Finally, Section VI details the conclusions of this study.

2.SYSTEM CONFIGURATION

a) Proposed Converter

Fig. 1 depicts a 4-phase dc-dc converter working in bidirection mode with interleave control .A unified PI voltage controller is used for controlling the switching pulses for each MOSFET switches. The objective of PI controller is to obtain a constant output voltage discounting the effect of variation in load. A complementary gating signal is provided by above mention controller. For interleave control switching pattern is adjusted by $2\pi/N$, where N is number of phase. The proposed converter is made to work in CCM (continuous conduction mode).

Journal of Engineering Sciences
Vol 10, Issue 9, Sept /2019
ISSN NO:0377-9254

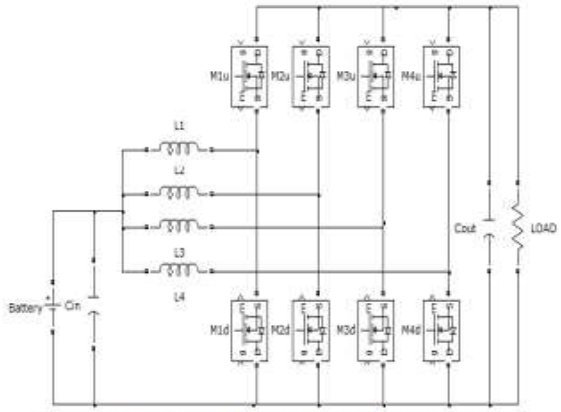

Fig. 1: Circuit of interleaved converter.

.

b) **Design of Converter:** Passive element (Inductors and capacitors) have a consequence impact of converters performance, efficiency and their size. Designing equations of bidirectional buck boost converters are given below:

$$\frac{V_{out}}{V_{in}} = \frac{D}{1-D} \quad (1)$$

$$C = \frac{I_{out} D}{2 f_s \Delta V_{out}} \quad (2)$$

$$L = \frac{V_{out} D T_s}{\Delta I_L} \quad (3)$$

Where L is the inductance, C is the capacitance, D is the duty ratio, Vout is the output voltage, Vin is the input voltage, s f is the switching frequency, Ts is the switching period, Δ L I is the inductor current ripple, ΔV out is the output voltage ripple.

3.CONTROL STRATEGY

(a) depicts the converter control structure, which consists of a vehicular strategic management level and the proposed BDC controller. The corresponding realized DSP flowchart for selecting operating modes of the proposed BDC is also shown in (b) for reference.

The strategic management level involves an electrical power demand estimation and contains a vehicular power and voltage management unit. The global results of the management must maximize the use of the source that best suits the power train power demand, fulfilling the driver and route requirements [21, 25-33]. In FCV/HEV power systems (Fig. 1), the dc-bus voltage of the driving inverter is regulated and powered by the FC stack through a dc-dc converter. Hence, instead of controlling the converter output voltage of each operation mode, the inductor current *iL*1 or *iL*2 is detected and compared with the reference current to control the power flow as shown in (a). In the converter control structure, the vehicular energy and power and voltage management unit selects the BDC mode according to the operating conditions of the vehicle, such as power demand of different driving state (*Pdem*) and the dual-source voltages (*VES*1, *VES*2). It then selects the appropriate current references *iL*1,*ref* or *iL*2,*ref* that can control the active switches (*S*, *Q*1~*Q*4) with proportional integral (PI) or more advanced methods. Notably, in spite of it is not easy to choose the optimal parameter of PI controller, the advantages of zero steady-state error and capability of noise filtering, making PI control the most widely used industry algorithm. Furthermore, referring to Table I, two switch selector (*x*1, *x*2) of BDC controller can be defined for various operating modes. The pulsed-width-modulation (PWM) switching scheme converts the duty cycle determined by different switch selector statuses into gate control signals for the power switches.

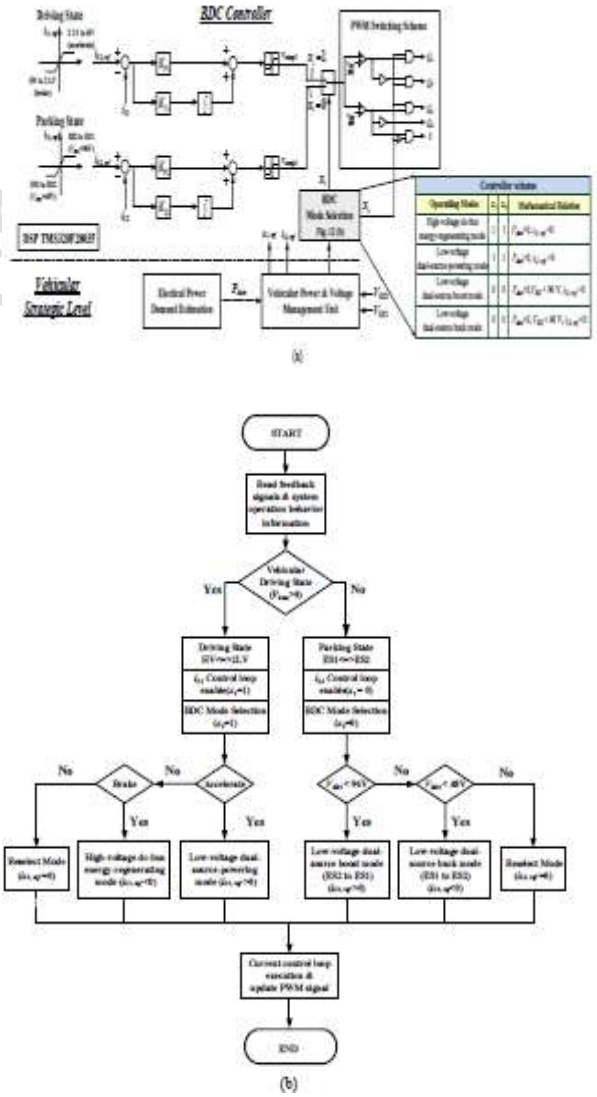

(a)Block diagram of the closed-loop control scheme; (b) realized DSP flowchart for various operating modes of the proposed BDC.

As (a) displays, the current reference *iL*1,*ref* is used to control the bidirectional power flow between the low-voltage dual-source and the high-voltage dc-bus (i.e., 2 LV to HV or HV to 2 LV). In either case, the average inductor current *iL*2 is equal to the controlled average inductor current *iL*1 because of the inherent uniform average current sharing in the proposed BDC topology. By contrast, the current reference *iL*2,*ref* is used to control the power flow between the main energy storage and the auxiliary energy storage (i.e., ES1 to ES2 or ES2 to ES1).

The procedure of mode switching is shown in (b) and it is depicted below. First of all, when vehicle is in driving state (*Pdem*>0), the controller is *iL*1 control loop (*x*1=1), and the controlled switches as shown in Table I (vehicle is accelerating (*iL*1,*ref* >0, HV to 2 LV) or braking (*iL*1,*ref* <0, 2 LV to HV)). If neither of the two situations, it will execute reselect mode to process the next judgement of mode switching. Additionally, when vehicle is in parking state (*Pdem*<0), the controller is *iL*2 control loop (*x*1=0), and controlled switches as shown in Table I. In this state, the judgement of mode switching depends on the voltage of *VES*1 (96 V) and *VES*2 (48 V). If *VES*1<96 V, the mode is low-voltage dual-source boost mode (*iL*2,*ref* >0, *VES*2 to *V*ES1). When *VES*2<48 V, the mode is low-voltage dual-source buck mode (*iL*2,*ref* <0, *VES*1 to *VES*2). If both situations do not be satisfied, it executes reselect mode to process the next

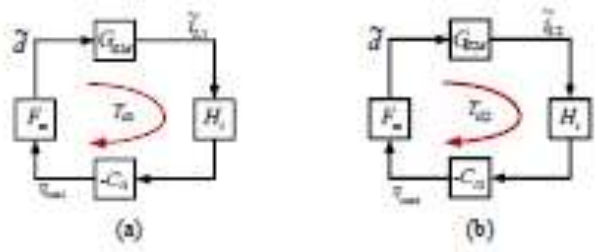

Block diagram of the closed-loop control scheme for (a) the low-voltage dual-source-powering and the high-voltage dc-bus energy-regenerating modes; (b) the low-voltage dual-source buck/boost mode.

judgement of mode switching. Only two closed-loop controllers were developed to control the four power flow conditions based on the average model of the proposed converter derived by using the state-space averaging technique. (a) shows the closed-loop control block diagram that is compatible with both low-voltage dual-source-powering boost mode (i.e., 2 LV to HV) and high-voltage dc-bus energy-regenerating mode (i.e., HV to 2 LV); the closed-loop control block diagram displayed in (b) is compatible with the low-voltage dual-source buck/boost mode (i.e., ES1 to ES2 or ES2 to ES1).

In Fig., *FM* represents the constant gain of the PWM generator; *GiL*1*d* denotes the transfer function, which converts the duty cycle to inductor current *iL*1; *GiL*2*d* is the transfer function from duty cycle to inductor current *iL*2; *Ci*1 and *Ci*2 represent the transfer function of inductor current controllers, and *Hi* is the sensing gain of the current sensor.

To design the closed-loop controller and simplify the mathematics of the proposed BDC, the PSIM© circuit model is built under the following three assumptions: 1) power switches and diodes are ideal; 2) equivalent series resistances of all inductors and capacitors of the converter are considered to obtain a relatively precise dynamic model; and 3) the converter is operated under a continuous conduction mode.

2)**Implementation Details:** In this section proposed converter design and cascaded with HEV MATLAB-SIMULINK model. The proposed converter is cascaded in between battery and PMSM (Permanent magnet synchronous motor). Converter is working in boost mode by providing a constant dc bus voltage of 500 V to PMSM and control SOC (state of charge) of battery during acceleration and deceleration mode of HEV. The specification of model used is listed in Table 1.

Table 1: System RATINGS

S. No		Power (KW)	Voltage (V)	Type
1.	Motor	50	500	8 Pole PMSM
2.	Generator	30	500	2 Pole PMSM
3.	Battery	21	200	Nickel Metal Hydride
4.	I.C.E	50	-	-

3) System Operation:

Mode 1

HEV at rest at initial position i.e. t=0 sec and simultaneously pushing the pedal 2/3rd of acceleration vehicles moves only through the electric motors being fed by battery only, if required power remaining below than 12KW.

Mode 2

The power requirement below than 12KW at time t=1.4 sec hybrid mode is triggered. The ICE and battery provides power to HEV through the motor. The generator and battery feeds power to motor. The acceleration is provided through this process.

Mode 3

At t=4 sec the acceleration is decreased slightly, the torque cannot be reduced by ICE alone therefore the generator is absorb by the battery.

Mode 4

At t=4.4 sec only battery provides power required by HEV and generator is stopped.

Mode 5

At t=8 sec ICE restart as acceleration is at nearly 4/5 of total, which provides the extra required power.

Mode 6

At t=13 sec acceleration is down to 2/3rd as in mode 1. The generator switches off in half a second. The motor runs generator this whole operation known as regenerative braking.

4.SIMULATION RESULT

Current in every inductor branch showed in Fig.2 Where average value of current is 27A and current ripples are very high. Peak to peak ripples as we see from, Fig is around ± 50A. This is quite high. In order to reduce the above mentioned ripples at the output interleave control is provided by phase shifted signal. Fig.3 shows the response of electrical system of used HEV model Fig.3 illustrates Output dc bus voltage, battery output voltage, SOC of battery, motor, generator and battery current in every above mentioned mode.

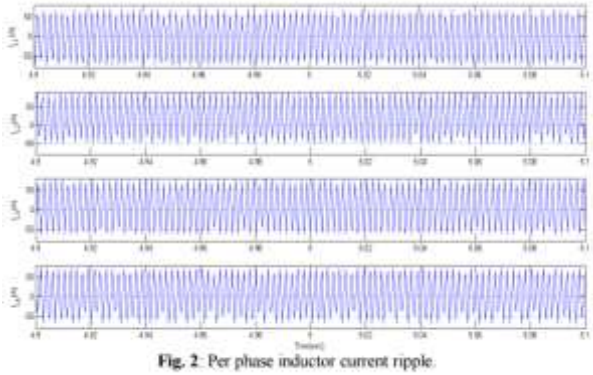

Fig. 2: Per phase inductor current ripple.

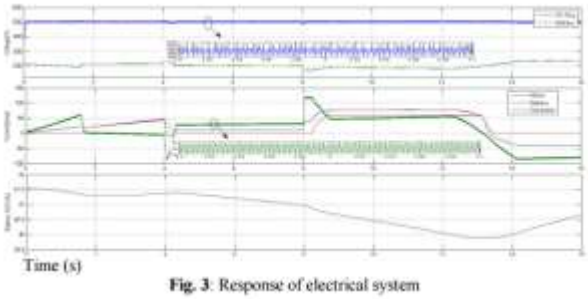

Fig. 3: Response of electrical system

The top graph of Fig.3 illustrates the output voltage of converter and output voltage of battery. Peak to peak output voltage ripples are ± 5V. Below graph of Fig.3 shows variations in motor, battery and generator current according to aforementioned operating modes of HEV. Average current is 27A and peak to peak ripples ±2A. This is quite low as compare to per phase inductor current. The last graph of Fig.3

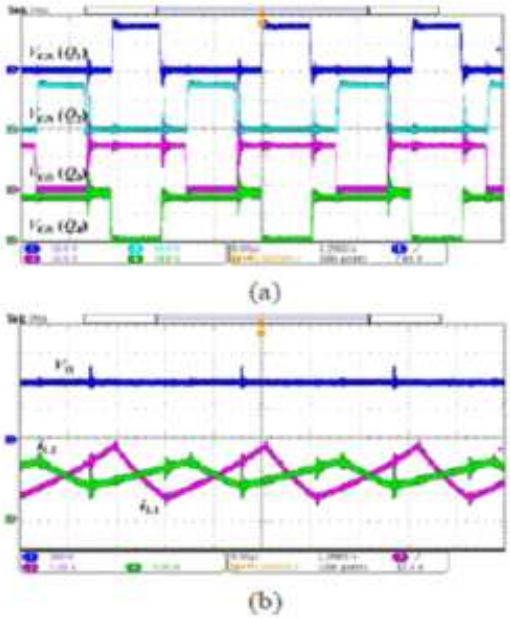

Fig.4. Measured waveforms for low-voltage dual-source-powering mode: (a) gate signals; (b) output voltage and inductor currents.

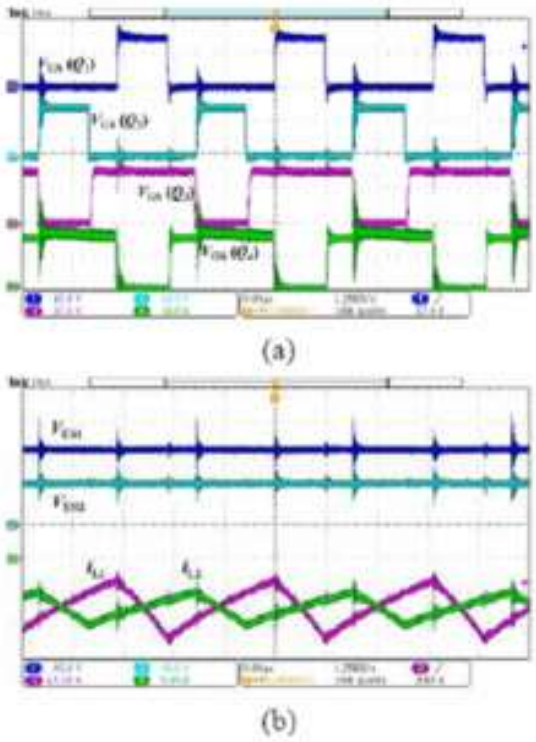

Fig.5. Measured waveforms for high-voltage dc-bus energy-regenerating mode: (a) gate signals; (b) output voltage and inductor currents.

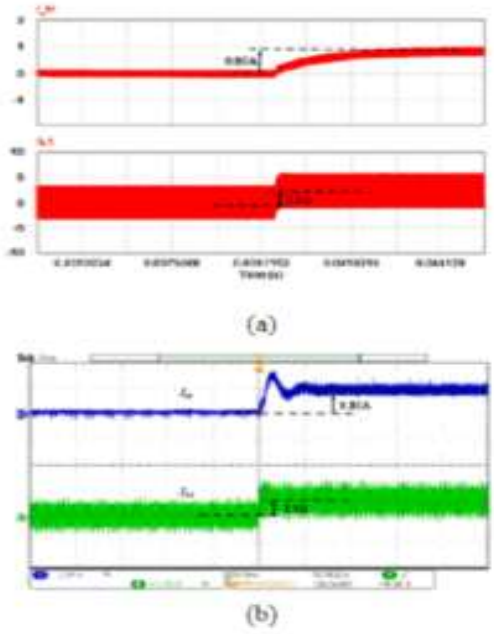

Fig.6. Measured waveforms of gate signals, output voltage and inductor currents for the low-voltage dual-source buck/boost mode: (a) buck mode; (b) boost mode.

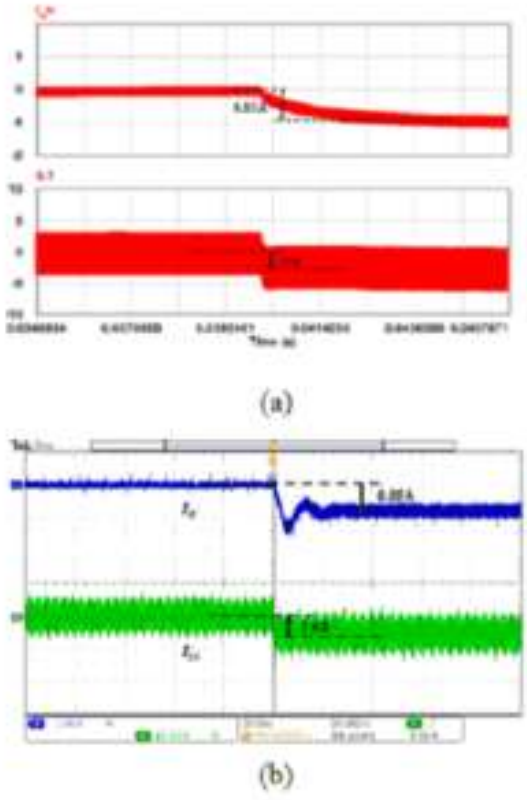

Fig. 7. Waveforms of controlled current step change in the low-voltage dual-source-powering mode: (a) by simulation; and (b) by measurement. (*iH* is changed from 0 to 0.85 A; *iL*1 is changed from 0 to 2.5 A; Time/Div=20 ms/Div)

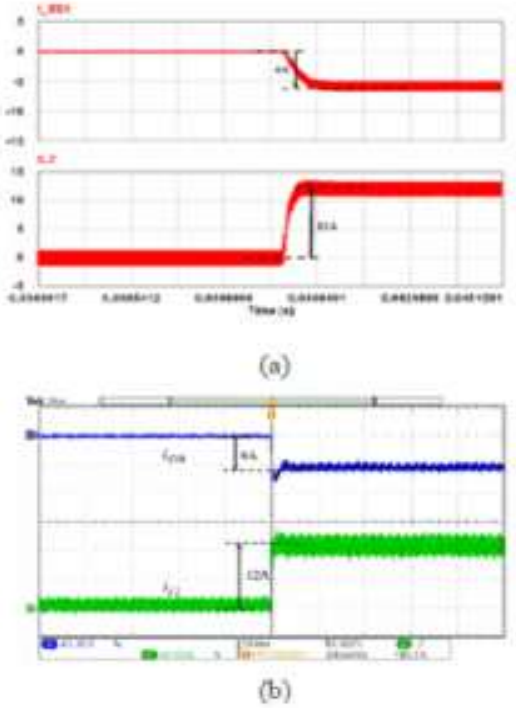

Fig. 8. Waveforms of controlled current step change in the low-voltage dual-source boost mode: (a) by simulation; and (b) by measurement. (*iES*1 is changed from 0 to -6 A; *iL*2 is changed from 0 to 12 A; Time/Div=20 ms/Div)

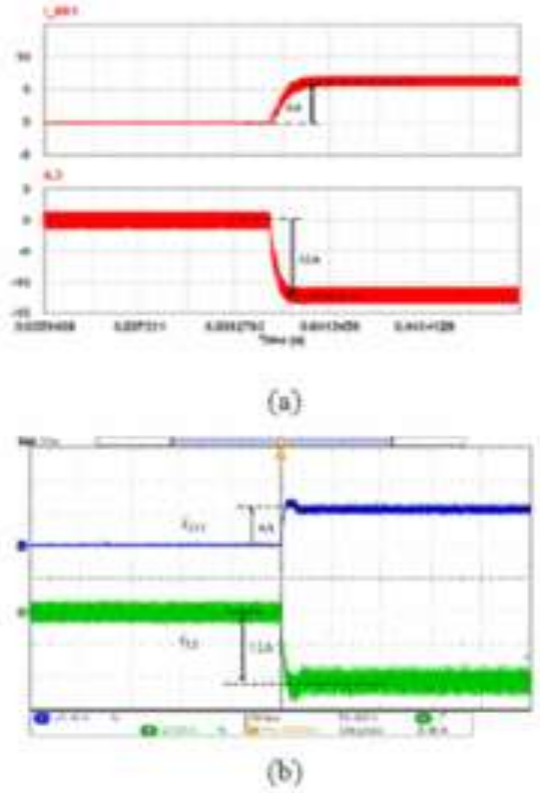

Fig. 9. Waveforms of controlled current step change in the low-voltage dual- source buck mode: (a) by simulation; and

(b) by measurement. (*iES*1 is changed from 0 to 6 A; *iL*2 is changed from 0 to 12 A; Time/Div=20 ms/Div)

shows state of charge (SOC) of the battery during charging and discharging mode as mentioned in above operating modes of HEV. Below table shows the comparison between bidirectional buck boost converter and proposed converter. It has been seen that size of passive component reduces considerably as compare to proposed converter.

Table 2: PARAMETER OF DC/DC CONVERTER

Item	Inductor [μH]	Capacitor [μF]	Switching Frequency [kHz]
Buck boost converter	98.7	72.87	40
Proposed converter	25.67	40.50	40
Reduction	73%	44.4%	-

5. CONCLUSIONS

A new BDC topology was presented to interface dual battery energy sources and high-voltage dc bus of different voltage levels. The circuit configuration, operation principles, analyses, and static voltage gains of the proposed BDC were discussed on the basis of different modes of power transfer. Simulation and experimental waveforms for a 1 kW prototype system highlighted the performance and feasibility of this proposed BDC topology. The highest conversion efficiencies were 97.25%, 95.32%, 95.76%, and 92.67% for the high-voltage dc-bus energy-regenerative buck mode, low-voltage dual-source-powering mode, low-voltage dual-source boost mode (ES2 to ES1), and low-voltage dual-source buck mode (ES1 to ES2), respectively. The results demonstrate that the proposed BDC can be successfully applied in FC/HEV systems to produce hybrid power architecture

REFERENCES

[1] M. Ehsani, K. M. Rahman, and H. A. Toliyat, "Propulsion system design of electric and hybrid vehicles," *IEEE Transactions on industrial electronics*, vol. 44, no. 1, pp. 19-27, 1997.

[2] A. Emadi, K. Rajashekara, S. S. Williamson, and S. M. Lukic, "Topological overview of hybrid electric and fuel cell vehicular power system architectures and configurations," *IEEE Transactions on Vehicular Technology*, vol. 54, no. 3, pp. 763-770, 2005.

[3] A. Emadi, S. S. Williamson, and A. Khaligh, "Power electronics intensive solutions for advanced electric, hybrid electric, and fuel cell vehicular power systems," *IEEE Transactions on Power Electronics*, vol. 21, no. 3, pp. 567-577, 2006.

[4] E. Schaltz, A. Khaligh, and P. O. Rasmussen, "Influence of battery/ultracapacitor energy-storage sizing on battery lifetime in a fuel cell hybrid electric vehicle," *IEEE Transactions on Vehicular Technology*, vol. 58, no. 8, pp. 3882-3891, 2009.

[5] P. Thounthong, V. Chunkag, P. Sethakul, B. Davat, and M. Hinaje, "Comparative study of fuel-cell vehicle hybridization with battery or supercapacitor storage device," *IEEE transactions on vehicular technology*, vol. 58, no. 8, pp. 3892-3904, 2009.

[6] C. C. Chan, A. Bouscayrol, and K. Chen, "Electric, hybrid, and fuel-cell vehicles: Architectures and modeling," *IEEE transactions on vehicular technology*, vol. 59, no. 2, pp. 589-598, 2010.

[7] A. Khaligh and Z. Li, "Battery, ultracapacitor, fuel cell, and hybrid energy storage systems for electric, hybrid electric, fuel cell, and plug-in hybrid electric vehicles: State of the art," *IEEE transactions on Vehicular Technology*, vol. 59, no. 6, pp. 2806-2814, 2010.

[8] K. Rajashekara, "Present status and future trends in electric vehicle propulsion technologies," *IEEE Journal of Emerging and Selected Topics in Power Electronics*, vol. 1, no. 1, pp. 3-10, 2013.

[9] C.-M. Lai, Y.-C. Lin, and D. Lee, "Study and implementation of a two-phase interleaved bidirectional DC/DC converter for vehicle and dc-microgrid systems," *Energies*, vol. 8, no. 9, pp. 9969-9991, 2015.

[10] C.-M. Lai, "Development of a novel bidirectional DC/DC converter topology with high voltage conversion ratio for electric vehicles and DC-micSrogrids," *Energies*, vol. 9, no. 6, p. 410, 2016.

[11] J. Moreno, M. E. Ortúzar, and J. W. Dixon, "Energy-management system for a hybrid electric vehicle, using ultracapacitors and neural networks," *IEEE transactions on Industrial Electronics*, vol. 53, no. 2, pp. 614-623, 2006.

[12] J. Bauman and M. Kazerani, "A comparative study of fuel-cell–battery, fuel-cell–ultracapacitor, and fuel-cell–battery–ultracapacitor vehicles," *IEEE Transactions on Vehicular Technology*, vol. 57, no. 2, pp. 760-769, 2008.

[13] M. Ehsani, Y. Gao, and A. Emadi, *Modern electric, hybrid electric, and fuel cell vehicles: fundamentals, theory, and design*. CRC press, 2009.

[14] Z. Haihua and A. M. Khambadkone, "Hybrid modulation for dual active bridge bi-directional converter with extended power range for ultracapacitor application," in *Industry Applications Society Annual Meeting, 2008. IAS'08. IEEE*, 2008, pp. 1-8: IEEE.

[15] H. Tao, J. L. Duarte, and M. A. Hendrix, "Three-port triple-half-bridge bidirectional converter with zero-voltage switching," *IEEE transactions on power electronics*, vol. 23, no. 2, pp. 782-792, 2008.

AUTHOR'S PROFILE:

[1]. M.RAVI KUMAR Pursuing his Masters Degree in Department of EEE from Kakinada Institute Of Technological Sciences (Kits), Ramachandrapuram.

[2]. DANDANGI RAMESH BABU , Completed his B.Tech Degree from Aditya Engineering College, Surampalem, Completed his M.Tech Degree from KITS Ramachandrapuram in EEE Department. Presently he is working as Assistant Professor in KITS Ramachandrapuram.. His Interested Area is Power Electronics.